

# Unusual Solid-State Behavior in a Neutral [2]Catenane Bearing a Hydrolyzable Component

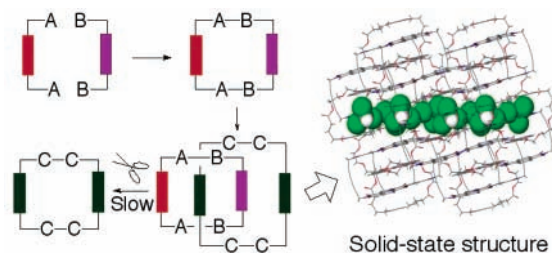
Gary D. Fallon, Marcia A.-P. Lee, Steven J. Langford,\* and Peter J. Nichols

School of Chemistry and Centre for Green Chemistry, Monash University,  
Clayton, Victoria 3800, Australia

steven.langford@sci.monash.edu.au

Received October 30, 2003

## ABSTRACT



A template-directed strategy to forming a bis(diimide) macrocycle through an intermediate asymmetric [2]catenane is reported. Saponification of the ester linkages within the crown ether component is much slower in the mechanically interlocked structure when compared to the free crown. The predominance of a single translational isomer leads to a dimeric structure, resulting in the generation of infinite channels within the crystal lattice.

Topological curiosities such as the [2]catenanes<sup>1,2</sup> have attracted much attention in the areas of materials science and nanotechnology<sup>3</sup> as a result of their ability to undergo translational isomerism upon the input of an external stimuli.<sup>4</sup> Ultimately, however, the use of catenanes in the fabrication

of useful materials and devices will lie in the control of their solid-state properties. The judicious choice of molecular instruction<sup>5</sup> programmed into each component within these mechanically interlocked molecules not only dictates the efficiency of the catenation process, the ratio and number of translational isomers present, and nature of the stimuli needed to switch between states but also the nature of the connectivity between individual molecular assemblies in the solid state. Hence new permutations of donors, acceptors, and linkers are useful in adding to the repertoire of aromatic-based catenanes for the generation of novel materials.

We have been interested in employing naphthalene diimides (NDIs) as analogues to bipyridinium- and diazapyrenium<sup>6</sup>-containing cyclophanes because of their neutral character, well-behaved redox properties, and chemical flexibility.<sup>2,7</sup> When we started this work, these types of

(1) (a) Schill, G. *Catenanes, Rotaxanes and Knots*; Academic Press: New York, 1971. (b) *Molecular Catenanes, Rotaxanes and Knots: A Journey Through the World of Molecular Topology*; Sauvage, J.-P., Dietrich-Buchecker, C., Eds.; Wiley-VCH: Weinheim, 1999.

(2) Amabilino, D. B.; Stoddart, J. F. *Chem. Rev.* **1995**, 95, 2725.

(3) (a) Yan, H.; Zhang, X.; Shen, Z.; Seeman, N. C. *Nature* **2002**, 415, 62. (b) Hanke, A.; Metzler, R. *Chem. Phys. Lett.* **2002**, 359, 22. (c) Asakawa, M.; Higuchi, M.; Mattersteig, G.; Nakamura, T.; Pease, A. R.; Raymo, F. M.; Shimizu, T.; Stoddart, J. F. *Adv. Mater.* **2000**, 12, 1099. (d) Langford, S. J.; Raymo, F. M.; Stoddart, J. F. In *Molecular Electronics*; Jortner, J., Ratner, M., Eds.; Blackwell Science: Oxford, 1997; p 325. (e) Colasson, B. X.; Dietrich-Buchecker, C.; Jimenez-Molero, M. C.; Sauvage, J.-P. *J. Phys. Org. Chem.* **2002**, 15, 476.

(4) (a) Balzani, V.; Credi, A.; Raymo, F. M.; Stoddart, J. F. *Angew. Chem., Int. Ed.* **2000**, 39, 3348. (b) Biscarini, F.; Cavallini, M.; Leigh, D. A.; Leon, S.; Teat, S. J.; Wong, J. K. Y.; Zerbetto, F. *J. Am. Chem. Soc.* **2002**, 124, 225. (c) Collier, C. P.; Jeppesen, J. O.; Luo, Y.; Perkins, J.; Wong, E. W.; Heath, J. R.; Stoddart, J. F. *J. Am. Chem. Soc.* **2001**, 123, 12632. (d) Balzani, V.; Credi, A.; Langford, S. J.; Stoddart, J. F. *J. Am. Chem. Soc.* **2000**, 122, 3542.

(5) Lehn, J.-M. *Supramolecular Chemistry*; VCH: Weinheim, Germany, 1995.

(6) (a) Credi, A.; Balzani, V.; Langford, S. J.; Stoddart, J. F. *J. Am. Chem. Soc.* **1997**, 119, 2679. (b) Credi, A.; Balzani, V.; Langford, S. J.; Montalti, M.; Raymo, F. M.; Stoddart, J. F. *New J. Chem.* **1998**, 1061.

The synthesis of the [2]catenane **6** (Scheme 1) requires the formation of the crown ether **4**, which was achieved in

Reaction scheme for the synthesis of macrocyclic ligands:

Starting material (4-hydroxyphenol) reacts with compound **1** ( $\text{Br}-\text{CH}_2\text{CH}_2\text{CH}_2\text{C}(=\text{O})\text{R}$ ) in the presence of  $\text{K}_2\text{CO}_3$  in MeCN under heating ( $\Delta$ ) to form compound **2** ( $\text{HO}-\text{C}_6\text{H}_4-\text{O}-\text{CH}_2\text{CH}_2\text{CH}_2\text{C}(=\text{O})\text{R}$ ).

Compound **2** is then treated with aq NaOH to yield two products:

- $\text{R} = \text{OCH}_2\text{CH}_3$ , 83% yield
- $\text{R} = \text{OH}$ , 75% yield

Compound **2** (with  $\text{R} = \text{OH}$ ) is further reacted with 1.  $(\text{COCl})_2$  / DMF / benzene /  $\text{N}_2$  and 2. **3** (a bis-phenol derivative) in benzene /  $\text{N}_2$  to form compound **4** (a macrocyclic ligand) in 32% yield.

Compound **4** is then reacted with compound **5** (a macrocyclic ligand) in the presence of CuCl and DMF to form the final macrocyclic ligand **6** (a macrocyclic ligand).

four steps from 1,4-hydroquinone and ethyl valerate. Two aspects of the design of **4** require mentioning. The first is that a valeric ester rather than a tetraethylene glycol group

At 300 K the 300 MHz  $^1\text{H}$  NMR spectrum of **6** in  $\text{CDCl}_3$  (Figure 1) differs greatly from the sum of the  $^1\text{H}$  NMR spectra of the two components (**4** + **5**) in multiplicity and

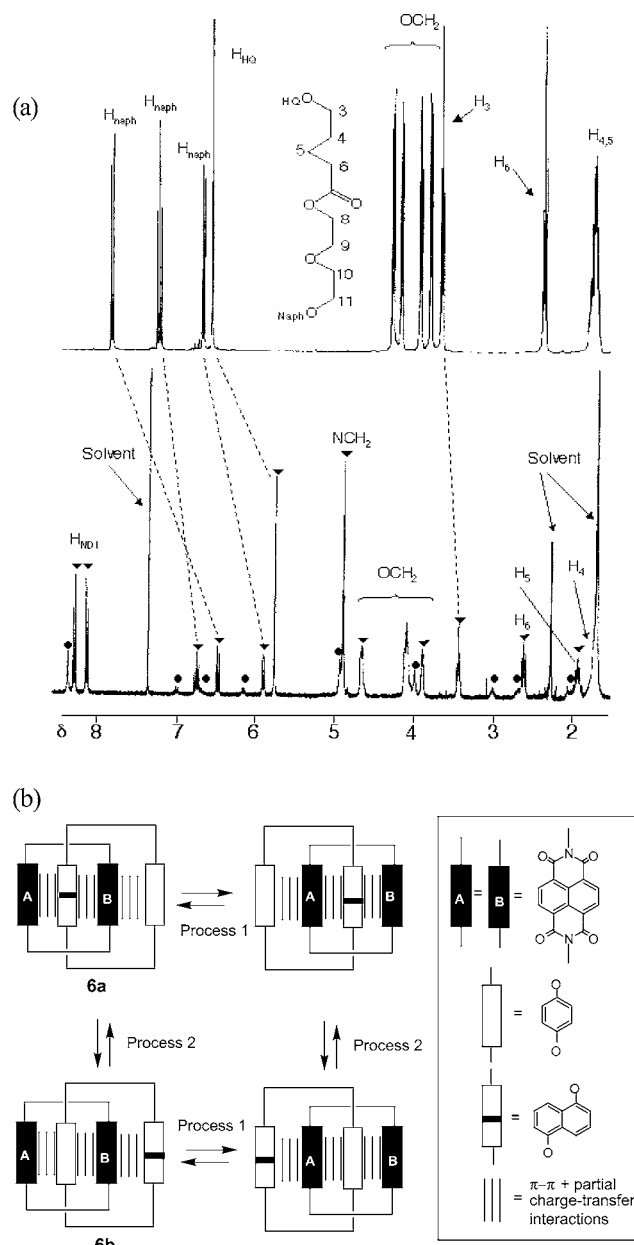


**Figure 1.** The 300 MHz  $^1\text{H}$  NMR spectra of (a) crown **4** (top) and the catenane **6** (bottom) in  $\text{CDCl}_3$  solution at 300 K. Key: **6a** ( $\blacktriangledown$ ) and **6b** ( $\bullet$ ). (b) A schematic representation of the two processes identified by  $^1\text{H}$  NMR spectroscopy.

(9) Hamilton, D. G.; Davies, J. E.; Prodi, L.; Sanders, J. K. M. *Chem. Eur. J.* **1998**, *4*, 608.

chemical shift. The spectrum is also complicated by two sets of signals (of different intensities) that are attributable to the two translational isomers **6a,b** resulting from the asymmetry in **4**. Integration of the relevant probe protons of both isomers indicates that at 300 K the ratio **6a:6b** is 4:1. This exchange between **6a** and **6b** is slow on the NMR time scale. Cooling the sample to 213 K causes a change in the ratio of **6a:6b** to 9:1, consistent with the expected bias toward the better recognition site in a lower energy environment.

At 300 K, the naphthalene diimide units within the major isomer **6a** exist as two doublets ( $\delta = 8.20$  and  $8.05$ ;  $^3J = 7.5$  Hz) in fast exchange between their respective positions inside and outside the cavity of **4** on the NMR time scale.<sup>14</sup> The doublet splitting pattern between the *ortho* protons of the NDI as well as the AB system centered at  $\delta$  4.81 ( $^2J = 13$  Hz at 288 K) attributable to the  $\text{NCH}_2$  protons is a result of the asymmetric environment induced by the 1,5-dioxonaphthalene unit in **4**. The resonances attributable to the  $-\text{OC}_6\text{H}_4-$  appear as a singlet at  $\delta$  5.68. The significant differences in chemical shifts ( $>0.5$  ppm) between resonances attributable to **4** and **6a** can be rationalized on the basis of the overlap between the aromatic units in both components (*vide infra*). This overlap of  $\pi$ -electron-rich and -deficient aromatic units is also responsible for the deep purple color of the sample. Heating a solution of the [2]-catenane **6** from 300 to 333 K leads to the identification of Process 2, which involves the circumrotation of the crown ether component through the diimide component. The difference in onset of this process between **6a** and **6b** ( $\Delta T = 15$  K) is a result of the different binding affinities between the hydroquinone and dioxonaphthalene units with respect to the NDI unit. This process is higher in energy than Process

1 as a result of the extra interactions that need to be overcome in this system to induce the process.

Dark purple single crystals of **6** suitable for X-ray analysis<sup>15</sup> were grown by vapor diffusion of hexane into chloroform solutions of **6**. The molecular structure of a dimer of **6a** is shown in Figure 2, and the macromolecular structure

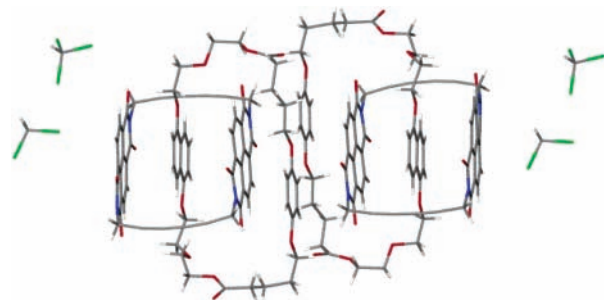


**Figure 2.** Schematic representation of that portion of the X-ray structure of **6a** illustrating the dimeric nature of the [2]catenane.

of the arrays formed by dimers of **6a** are shown in Figure 3. The solid-state structure of the [2]catenane shows the 1,5-dioxonaphthalene of the crown ether **4** to be positioned inside the cavity of the newly formed bis-NDI macrocycle. This is consistent with the  $^1\text{H}$ NMR studies over the range 200–300 K. The [2]catenane is stabilized by  $[\pi\cdots\pi]$  interactions

(10) For discussion of template-directed syntheses, see: Anelli, P.-L.; Ashton, P. R.; Ballardini, R.; Balzani, V.; Delgado, M.; Gandolfi, M. T.; Goodnow, T. T.; Kaifer, A. E.; Philp, D.; Pietraszkewicz, M.; Prodi, L.; Reddington, M. V.; Slawin, A. M. Z.; Spencer, N.; Stoddart, J. F.; Vicent C.; Williams, D. J. *J. Am. Chem. Soc.* **1992**, *114*, 193 and references therein.

(11) Hamilton, D. G.; Feeder, N.; Prodi, L.; Teat, S. J.; Clegg, W.; Sanders, J. K. M. *J. Am. Chem. Soc.* **1998**, *120*, 1096.

(12) This methodology has been employed previously in a [3]catenane; see: Asakawa, M.; Ashton, P. R.; Menzer, S.; Raymo, F. M.; Stoddart, J. F.; White, A. J. P.; Williams, D. J. *Chem. Eur. J.* **1996**, *2*, 877.

(13) **Selected Spectroscopic Data. Data for 4:**  $^1\text{H}$  NMR (300 MHz,  $\text{CDCl}_3$ )  $\delta$  7.82 (d,  $J$  8.6 Hz, 2H, NQ-H), 7.25 (dd,  $J$  7.6, 8.6 Hz, 2H, NQ-H), 6.73 (d,  $J$  7.6, 2H, NQ-H), 6.59 (s, 4H, HQ-H), 4.32 (t,  $J$  3.0 Hz, 4H,  $\text{OCH}_2$ ), 4.22 (t,  $J$  3.0 Hz, 4H,  $\text{OCH}_2$ ), 3.97 (t,  $J$  3.0 Hz, 4H,  $\text{OCH}_2$ ), 3.84 (t,  $J$  3.0 Hz, 4H,  $\text{OCH}_2$ ), 3.71 (t,  $J$  6.0 Hz, 4H,  $\text{OCH}_2\text{CH}_2\text{CH}_2$ ), 2.39 (t,  $J$  7.0 Hz, 4H,  $\text{CH}_2\text{CO}$ ), 1.80–1.72 (m, 8H,  $\text{OCH}_2\text{CH}_2\text{CH}_2$ );  $^{13}\text{C}$  NMR (75 MHz,  $\text{CDCl}_3$ )  $\delta$  173.4, 154.2, 152.8, 126.6, 125.1, 115.2, 105.6, 69.6, 69.3, 67.7, 67.6, 63.4, 33.9, 28.3, 21.9; ESIMS (+ive)  $m/z$  633  $[\text{M} + \text{Na}]^+$ . **Data for 6a:**  $^1\text{H}$  NMR (300 MHz,  $\text{CDCl}_3$ )  $\delta$  8.18 (d,  $J$  7.56 Hz, 4H, NDI-H), 8.06 (d,  $J$  = 7.52 Hz, 4H, NDI-H), 6.66 (t,  $J$  7.91 Hz, 2H, NQ-H), 6.41 (d,  $J$  = 8.25 Hz, 2H, NQ-H), 5.83 (d,  $J$  = 7.5 Hz, NQ-H), 5.68 (s, 4H, HQ-H), 4.81 (s, 8H,  $\text{NCH}_2$ ), 4.57 (d,  $J$  3.9 Hz, 4H,  $\text{OCH}_2$ ), 4.03–3.98 (q, 8H,  $\text{OCH}_2$ ), 3.80 (d,  $J$  4.9 Hz, 4H,  $\text{OCH}_2$ ), 3.50 (t,  $J$  6.2 Hz, 4H,  $\text{OCH}_2\text{CH}_2\text{CH}_2$ ), 2.52 (t,  $J$  7.9 Hz, 4H,  $\text{CH}_2\text{CO}$ ), 1.83 (t,  $J$  7.7 Hz, 4H,  $\text{OCH}_2\text{CH}_2\text{CH}_2$ ), 1.62 (t,  $J$  8.3 Hz, 4H,  $\text{OCH}_2\text{CH}_2\text{CH}_2$ );  $^{13}\text{C}$  NMR (75 MHz,  $\text{CDCl}_3$ )  $\delta$  173.6, 161.6, 161.4, 152.2, 152.0, 150.5, 130.5, 130.0, 125.7, 125.3, 125.1, 124.9, 124.4, 123.2, 114.3, 113.6, 111.0, 104.3, 69.9, 68.2, 66.9, 64.2, 34.1, 30.4, 30.1, 29.7, 28.4, 22.4; ESIMS (+ive)  $m/z$  1291  $[\text{M} + \text{H}]^+$ , 1313  $[\text{M} + \text{Na}]^+$ , 1329  $[\text{M} + \text{K}]^+$ .

(14) The process is most likely a circumrotation of the hydroquinone unit around the periphery of the NDI macrocycle, which requires the interruption to only one set of interactions. A broadening of the resonances attributable to the alkyl groups of component **4** below 220 K is consistent with the slowing down of this process on the NMR time scale.

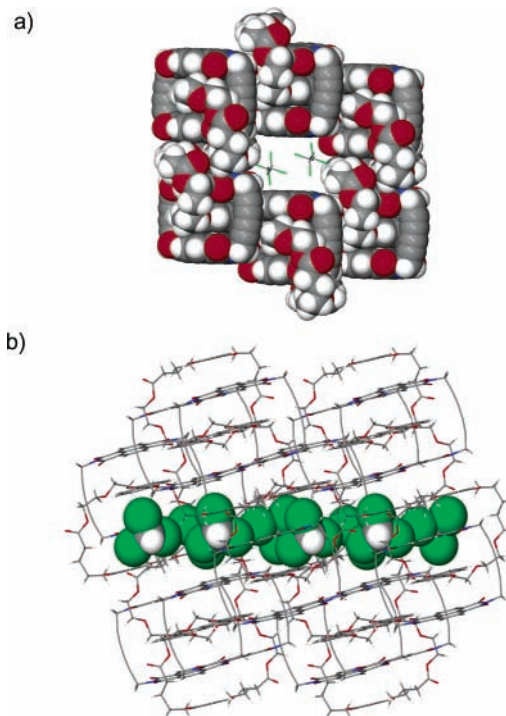


**Figure 3.** (a) A perspective view of the porous framework of an array of **6a** down the crystallographic *a*-axis showing regular channels, and (b) a view proximal to the *c*-axis.

between the planes of the four aromatic rings, giving rise to regular distances of 3.4 Å between each aromatic plane. Two notable features of the crystal structure are (a) the offset orientation of the hydroquinone ring with respect to the three other aromatic components and (b) the proximity of chloroform solvent molecules with respect to the outside NDI unit (NDI...Cl closest distances = 3.4, 3.6 Å). Further inspection reveals that the catenane resides in a dimeric structure displaying an unusual polar stacking motif in which the two offset hydroquinone units within the dimer yield an aromatic plane that interacts with the two inside NDI units within the two respective [2]catenanes. The result is a peculiar donor (D)–acceptor (A) stack (represented by A...D<sub>s</sub>...A...(D<sub>w</sub>UD<sub>w</sub>)...A...D<sub>s</sub>...A; s = stronger  $\pi$ -electron donor, w = weaker  $\pi$ -electron donor) terminated by chloroform solvent molecules. The packing of the hydroquinone units is almost zipperlike, though no significant interactions between the ester linkages within the crown component occur. There is, however, a strong interaction between a carbonyl group within component **4** and a chloroform molecule, giving rise to a C=O...Cl distance of 2.82 Å.

A view down the crystallographic *a*-axis shows that the [2]catenane array has an extremely open structure (Figure 3) dominated by a hydrophobic cavity. The chloroform molecules within the channels are ordered and packed in such a way that they alternate in order to maximize the Cl...Cl contacts (distances = 3.4–3.9 Å). The solid-state structure of **6** differs from the numerous [*n*]catenane structures in that the common D...A...D...A...D pattern is not observed. This example illustrates a potential to fine-tune not only the translational isomerism within but also the solid-state behavior of a [2]catenane.

A comparison of the rates of hydrolysis of **6** against **4** (excess 35% (v/v) aqueous DCl in CD<sub>3</sub>CO<sub>2</sub>D/CDCl<sub>3</sub>)<sup>16</sup>

(15) **Crystal data for 6:** C<sub>76</sub>H<sub>60</sub>C<sub>16</sub>N<sub>4</sub>O<sub>18</sub>, MW = 1529.98, crystal dimension 0.25 × 0.17 × 0.04 mm<sup>3</sup>, *a* = 1479.49(4), *b* = 16.3844(3), *c* = 17.3132(5) Å,  $\alpha$  = 65.941(2),  $\beta$  = 70.501(1),  $\gamma$  = 63.985(2), triclinic *P*-1, *Z* = 2, *V* = 3381.96(15) Å<sup>3</sup>,  $\rho_{\text{calc}}$  = 1.502 Mg m<sup>-3</sup>, *F*(000) = 1580,  $\lambda$  = 0.71073 Å, *T* = 123(2) K,  $\mu$  = 0.334 mm<sup>-1</sup>, Norius Kappa CCD diffractometer,  $\phi$  scan data, 63428 data collected, corrected for Lorentz and polarization effects, 16404 unique (*R*<sub>int</sub> = 0.115) and 16404 observed [*I* > 2 $\sigma$ (*I*)], 937 refined parameters, *R* = 0.0660, *R*<sub>w</sub> = 0.1201, *w* = ( $\sigma^2(F)$ )<sup>-1</sup>. Crystallographic data (excluding structure factors) for **6** has been deposited with the Cambridge Crystallographic Data Centre as supplementary publications no. CCDC-220655. Copies of the data can be obtained free of charge on application to CCDC, 12 Union Road, Cambridge CB21EZ, UK (fax (+44)1223-336-033; e-mail deposit@ccdc.cam.ac.uk).

illustrates the effectiveness of the [2]catenane to resist degradation. The ester linkages in the crown **4** are hydrolyzed in >85% in 24 h at 300 K by <sup>1</sup>H NMR spectroscopy. In contrast, the [2]catenane is <20% hydrolyzed after 260 h under these same conditions. Electrospray ionization mass spectrometry confirms that hydrolysis is taking place within the [2]catenane. The ESI mass spectrum of **6** is dominated by peaks at *m/z* 1291 ([**6** + H]<sup>+</sup>, 20%), 1313 ([**6** + Na]<sup>+</sup>, 100%), and 1329 ([**6** + K]<sup>+</sup>, 40%) and a signal at *m/z* 611 ([**4** + H]<sup>+</sup>, 80%). Upon exposure to the reaction conditions described above the intensity of the signals changes (**4**:**6**<sub>initial</sub> = 1:2; **4**:**6**<sub>final</sub> = 2:1) and a new signal at *m/z* 681 ([**6**–**4** + H]<sup>+</sup>, 10%) appears. This new signal is attributable to the desired bis-NDI cyclophane. The differences in reactivity between **4** and **6** can be accounted for by two factors. The mechanically interlocked nature of **6** combined with the dynamic processes undertaken by the two rings (Figure 1b) may create a situation whereby steric problems exist for the incoming reagents. The ability of **4** to act as a better phase transfer agent under the conditions employed may also play an important role. Whatever the mechanisms involved, the resistance of **6** to hydrolysis may provide a useful approach to slow-release drug delivery.

In conclusion we have synthesized a novel [2]catenane that exhibits unusual solid-state behavior. A proof-of-concept to forming cyclophanes using [2]catenanes as a precursor has also been illustrated.

**Acknowledgment.** This work was supported in part by the Australian Research Council's Discovery Scheme and through the Special Research Centre for Green Chemistry (scholarship to M.A.-P.L.).

**Supporting Information Available:** Experimental procedures and characterization for compounds **2**, **4**, and **6**. This material is available free of charge via the Internet at <http://pubs.acs.org>.

OL036116S

(16) CD<sub>3</sub>CO<sub>2</sub>D was necessary as the solvent in order to solubilize the [2]catenane **6** under the reaction conditions. The solubility problems of the catenane are inherent in the bis(diimide) macrocycle, which has been difficult to isolate. It seems that isolation of these macrocycles in any useful quantity will require the catalytic reduction of the acetylenic bridging groups to improve the solubility.